BILINGUAL PUBLISHING CO.
Pioneer of Global Academics Since 1984

Journal of Electronic & Information Systems
https://ojs.bilpublishing.com/index.php/jeis

ARTICLE

Wireless Power Transfer for 6G Network Using Monolithic Components on GaN

Rajinikanth Yella[1*] Krishna Pande[2] Ke Horng Chen[2]

1. Electrical Engineering Computer Science (EECS), NCTU, Taiwan, China
2. Electrical Engineering (EE), NCTU, Taiwan, China

ARTICLE INFO

Article history
Received: 11 August 2021
Accepted: 20 August 2021
Published Online: 30 August 2021

Keywords:
Wireless power transfer
Antenna
Rectifier
Filter

ABSTRACT

A novel architecture for Wireless Power Transfer (WPT) module using monolithic components on GaN is presented in this paper. The design of such a WPT module receives DC power from solar panels, consists of photonic power converter (PPC), beamforming antenna, low pass filter, input matching network, rectifier, output matching network and logic circuit (off-chip) which are all integrated on a GaN chip. Our WPT components show excellent simulated performance, for example, our novel beam-forming antenna and multiple port wideband antenna have a gain of 8.7 dB and 7.3 dB respectively. We have added a band pass filter to the rectifier output which gives two benefits to the circuit. The first one is filtering circuit will remove unwanted harmonics before collecting DC power and second is filter will boost the efficiency of rectifier by optimizing the load impedance. Our proposed rectifier has RF-DC conversion efficiency of 74% and 67% with beam-forming antenna and multiple port wide band antenna respectively. Our WPT module is designed to charge a rechargeable battery (3 V and 1 mA) of a radio module which will be used between two antennas in future 5G networks. We believe our proposed WPT module architecture is unique and it is applicable to both microwave and millimeter wave systems such as 6G.

1. Introduction

In the last few years, a silent but quite dramatic, a revolution occurred in the development and production of autonomous electronic devices (e.g. laptops, smart phones, palm pilots, digital cameras, household robots, networked radios, base stations, etc.) that we use in our daily life. Currently, batteries power most of these devices and their disposal is environmental disaster. In future for energy transmission between two antennas repeater radios will be used [1] as shown in Figure 1, which are needed to be charged wireless because these radios will be deployed mostly in rural areas. This fact motivated us to think of solution that could enable wireless power transfer (WPT) using RF energy harvesting techniques to such devices.

Our WPT module is designed to charge a rechargeable battery (3 V and 1 mA) of a radio module. Existing techniques [2-5] (such as near-field inductive coupling, magnetic resonant coupling) for wireless power transfer allow transmission of tens of watts of power over a few meters. However, such techniques suffer from low efficiency and a smaller range. Here, we report the design of a WPT module using novel monolithic components on GaN at 5.8 GHz frequency (ISM band 4) that has potential to convert

**Corresponding Author:*
Rajinikanth Yella,
Electrical Engineering Computer Science (EECS), NCTU, Taiwan, China;
Email: rajini.02g@g2.nctu.edu.tw

 DOI: https://doi.org/10.30564/jeisr.v3i1.3549

the power efficiently and transfer the power to devices deployed in remote areas. Our research goal and its implementation are to maximize the distance of power transfer and to achieve maximum conversion efficiency.

An overview of the architecture and components for our proposed WPT module on a GaN chip is shown in Figure 1. The Integrated Chip (Figure 1) consist of various individual components such as; (i) Beamforming Antenna; (ii), Solar power feed to antenna; (iii) Photonic Power Converters, (iv) Filter; (v) Input matching circuits (vi) Rectifier, diode sensor (vi) and digital control circuit.

This paper only deals with the optimum design of individual components. It can be observed that sunlight striking on solar panel gives DC energy signal which is converted to photonic signal by PPC. The antenna acts as a transducer between PPC to decrease losses. A low pass filter will allow the signal to pass with a frequency lower than 5.8 GHz. It will then be converted to RF power signal by using rectifier. The sensor is used to check the correct device bias voltage and impedance of the rectifier.

Figure 2 shows proposed basic building blocks of the on-chip GaN WPT module. In the future, we will extend our proposed technologies to millimeter (mm) wave frequency, as there are several motivations to use mm-wave frequencies in radio links such as availability of wider bandwidth, relatively narrow beam widths, better spatial resolution and small wavelength allowing modest size antennas to have a small beam width.

The physical dimension of antennas becomes so compact that it good on practical to build complex antenna arrays integrate them on-chip. In this paper, we are presenting the design of the monolithic WPT module containing components from antenna to load as shown in Figure 2 is presented. The goal is to ultimately fabricate the monolithic WPT on GaN substrate

2. Photonics Power Converter (PPC)

In order to reduce losses in the WPT module, for remote device application a number of modules connected together of photonic power converter (PPC) can be used

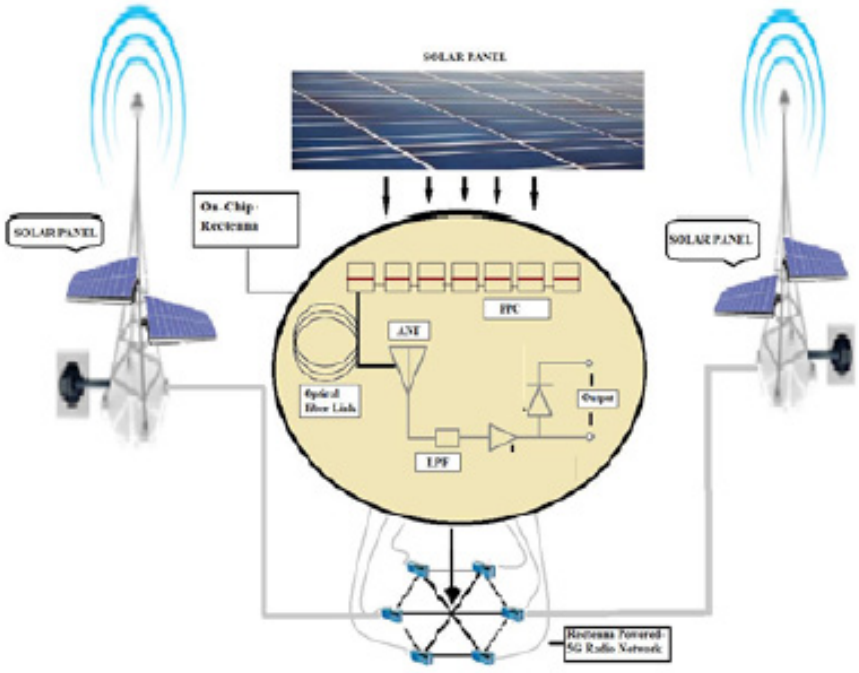

Figure 1. Proposed technology of WPT for 5G Network Communication

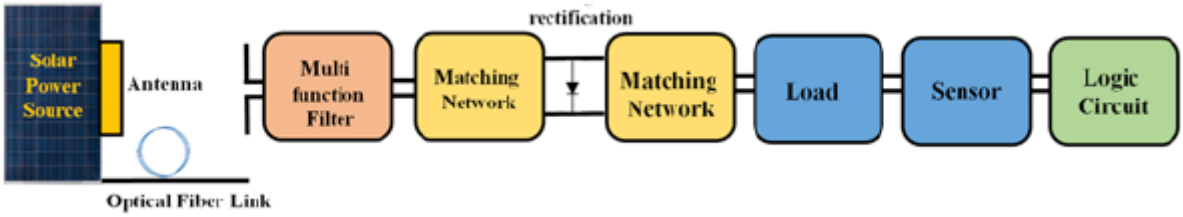

Figure 2. Proposed basic building blocks of WPT on same GaN chip

DOI: https://doi.org/10.30564/jeisr.v3i1.3549

for converting DC power to photonic into Electrical power, although PPCs are not required. So far for the photonic converters GaAs and Si materials have been used with optimization for absorption a different wavelength. For high conversion efficiencies GaAs has demonstrated 5. However, GaN is more suitable for PPC as it has wide bandgap, large breakdown voltage, and high electron saturation velocity. As shown in Figure 1, power from Solar cells will be launched into a photonic power converter (PPC) which will be a less than 2x2 mm GaN chip. To add voltages from the junctions several HEMT diodes connected in series, the amount of delivered current is proportional to the level of light power from solar cells illuminating the chip. PPC can be coupled with 980 nm fiber to transform the DC signal and finally expect to convert optical to electrical power. Our proposed idea, GaN photonic converter is expected to generate greater than 5 volts using a monolithic device chain. We expect optical-to-electrical power efficiency greater than 90% for the GaN PPC chip.

3. Antenna Design

Traditionally, antennas are off-chip due to their size and because typical substrates are conductive. However, if the antenna can be realized on-chip, it can result in a fully integrated system at a low cost. Monolithic Si-based integrated antennas have been demonstrated in recent years. However, standard silicon substrate is loss due to its low substrate resistivity, typically less than 100 cm. Moreover, the high dielectric constant of silicon causes most of the power to be absorbed in the substrate. This is a major drawback for antenna implementation on-chip, as it does not allow the energy to radiate efficiently into free space.

The mm-wave communication is widely accepted as a promising candidate for fifth and sixth generation (5G/6G) mobile communication systems 6 in order to handle massive data demand. According to the Friis transmission equation 7, by increasing the operation frequency, the signal wavelength becomes shorter and the path loss increases. Hence, in order to get the required gain overcoming attenuation effects, physically smaller antennas arranged as an array are desired.

In this paper, we are proposing two different kinds of on-chip GaN antennas for improvement in the radiation efficiency and gain using novel element design, the first one is beamforming array antenna (BFAA) and second one is multiple port wideband antenna (MPWBA). The true advantage of on-chip antenna can be attained by its realization in GaN chip process so that the circuits can be integrated with the back end digital blocks on the same chip because GaN will provide low loss, wide bandwidth, favorable linear polarization, and temperature stability [8-10].

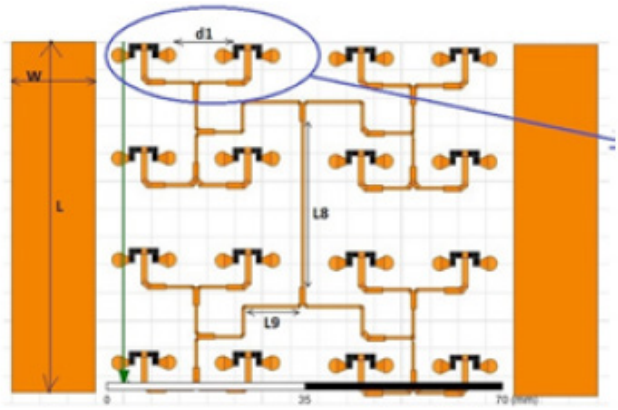

(a)

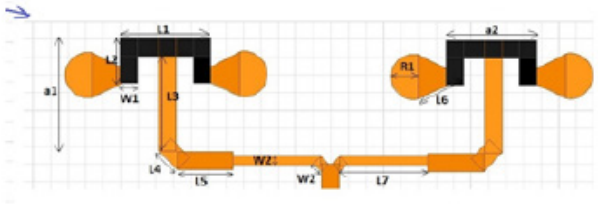

(b)

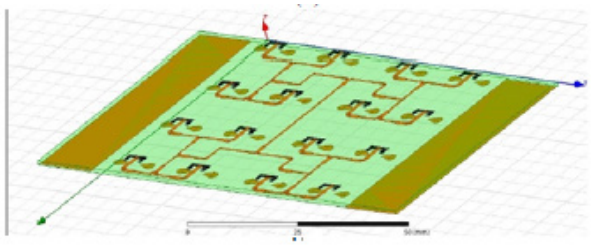

(c)

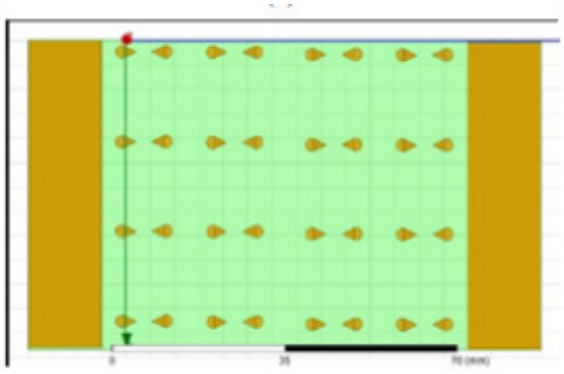

(d)

Figure 3. (a) Geometry of the proposed 4 X 4 antenna elements (b) single element (c) top view (d) bottom view

4. Beamforming Array Antenna (BFAA)

Generally, antenna arrays are used to generate a high gain. The antenna gain is proportional to its effective area.

DOI: https://doi.org/10.30564/jeisr.v3i1.3549

The higher antenna gain corresponds to the larger effective area and receives more electromagnetic power. One of the important parameters of array design, which must be accommodated very carefully, is set-out of the distance between the adjacent elements of an array. The decrement and increment in distance cause interference and distortion, not allowing further assessment of received signals [11]. Many mutual coupling reduction techniques have been proposed to improve the isolation performance between the antenna elements, such as neutralization line technology [12], electromagnetic bandgap [13-17], mush-room like decoupling structures [16] and meta-material decoupling [18,17,20]. By using these decoupling structures, isolation can be improved.

In this paper, we are proposing a two-layer beamforming a 4x4 array antenna with high isolation between elements. We have used high-frequency structure simulator (HFSS), full-wave solver, to design the antenna. The top layer is a T shape structure and bottom layer consists of drum type elements as shown in Figure 3a. For beamforming array, the distance between antenna elements is kept close to λ /4. Line length is adjusted to create delay between adjacent elements for beamforming radiation patterns. Dimensions of proposed antenna are mentioned in Table 1 (all dimensions in the Table 1 are in mm). The orange color in Figure 3a is gold material, yellow color is GaN material and light green color is GaN substrate.

Table 1. Dimensions of the proposed antenna

L	63	L5	3.2	W	15	a1	6.3
L1	5.2	L6	6.2	W1	1	a2	11.5
L2	2.5	L7	7.5	W2	0.5		
L3	5.3	L8	8.3	R1	1.5		
L4	1.5	L9	9.1	D1	7		

The configuration of our designed antenna array is shown in Figure 3. The antenna is comprised of T shaped with butterfly/drum-shaped patch elements. GaN was used as substrate while simulating antenna array. The substrate details which we used while simulating are, thickness of substrate is 1 mm, loss tangent value is 0 and relative permittivity is 9.7. The top layer is a T-shaped stub structure that is embedded in the GaN substrate, which has a distance of 0.1mm to the top surface of the substrate. The bottom layer is comprised of two inverted drum-shaped patches, which is embedded in the GaN substrate with a distance of 1 mm to the bottom of the GaN substrate.

The Figure 4 depicts the S11 response of the proposed antenna. The simulated S11 graph has -10 dB return loss from 5.67- 5.93 GHz, which means bandwidth of antenna is nearly 0.26 GHz. To overcome the performance degradation caused by beamforming usually we have to maintain mutual coupling between elements. In this paper we have maintained -30 dB.

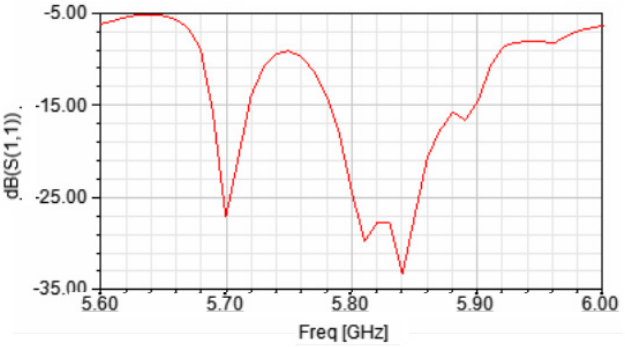

Figure 4. Return loss (S11) of BFAA

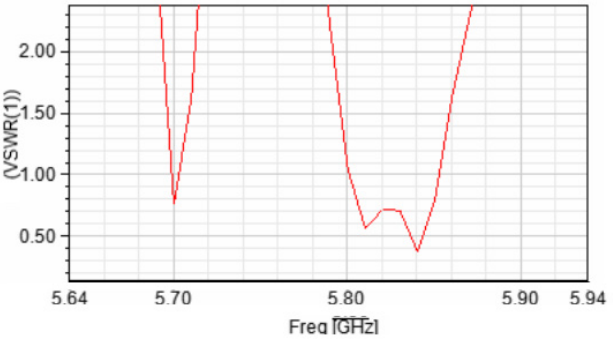

Figure 5. VSWR of BFAA

The Figure 5 shows VSWR (voltage standing wave ratio) of the antenna, usually for a good antenna VSWR should be below 2. Our simulation shows that for the passband frequency, antennas VSWR is below 1.2 as in Figure 5.

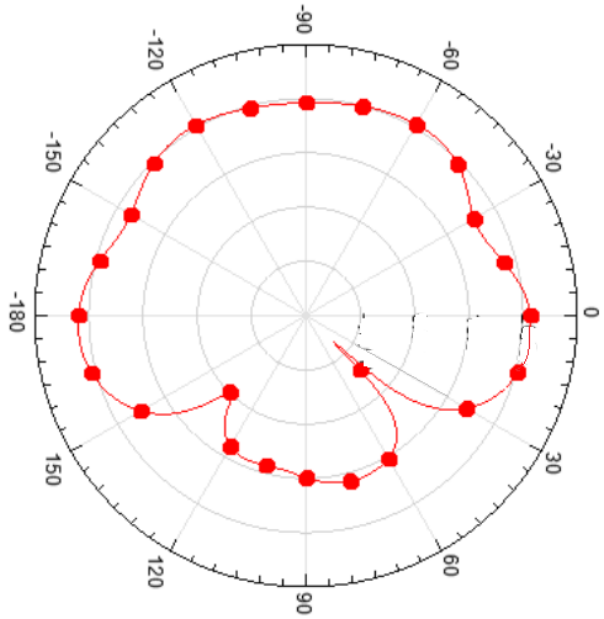

Figure 6. Radiation pattern of proposed antenna YZ plane

DOI: https://doi.org/10.30564/jeisr.v3i1.3549

The Figure 6 and Figure 7 are radiation patterns in YZ and XZ directions respectively. The patterns on the Smith chart indicate stability, low loss, and nearly ideal response.

The proposed BFAA 3D radiation pattern is shown in Figure 8. Our proposed antenna has maximum gain of 8.7 dB. From different angles, the proposed antenna has high gain, the overall antenna gain from 0° to 180° degree, ranges from 8.2 to 8.6 dB.

It is observed from the Figure 9 that the proposed antenna is maintaining good range current whole structure.

4.1 Design of Multiport Wide Band Antenna (MPWBA)

In our proposal, we also plan, alternately, to integrate multiport wideband antenna (MPWBA) on GaN chip for the

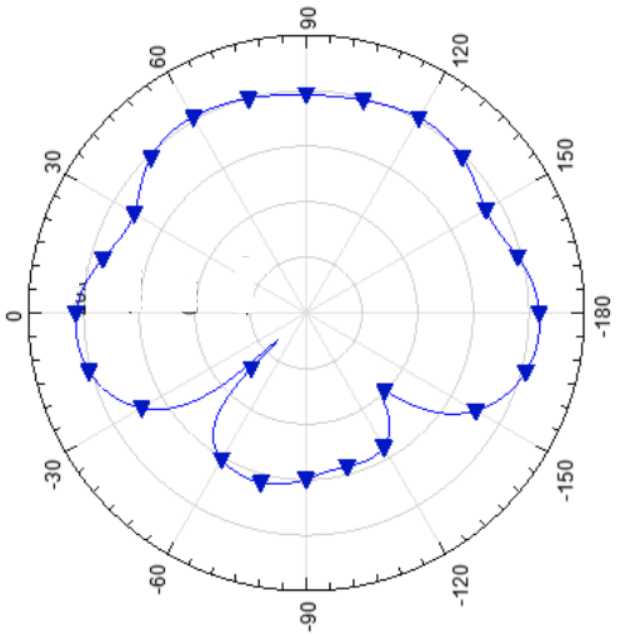

Figure 7. Radiation pattern of proposed antenna XZ plane

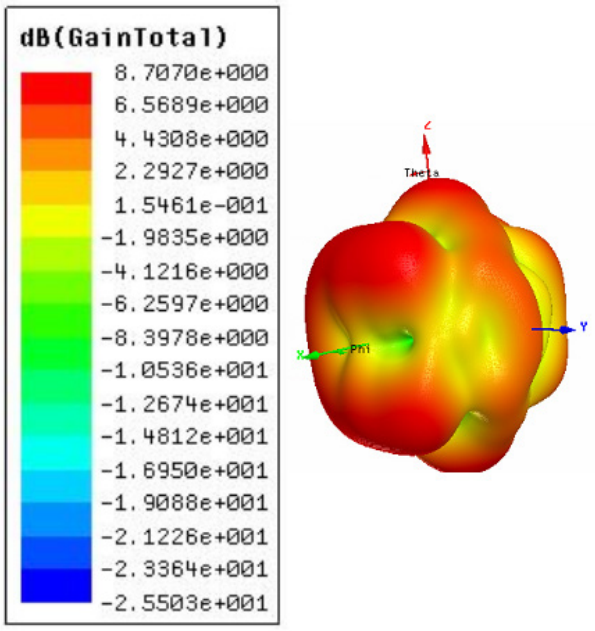

Figure 8. The 3D radiation pattern of proposed BFAA

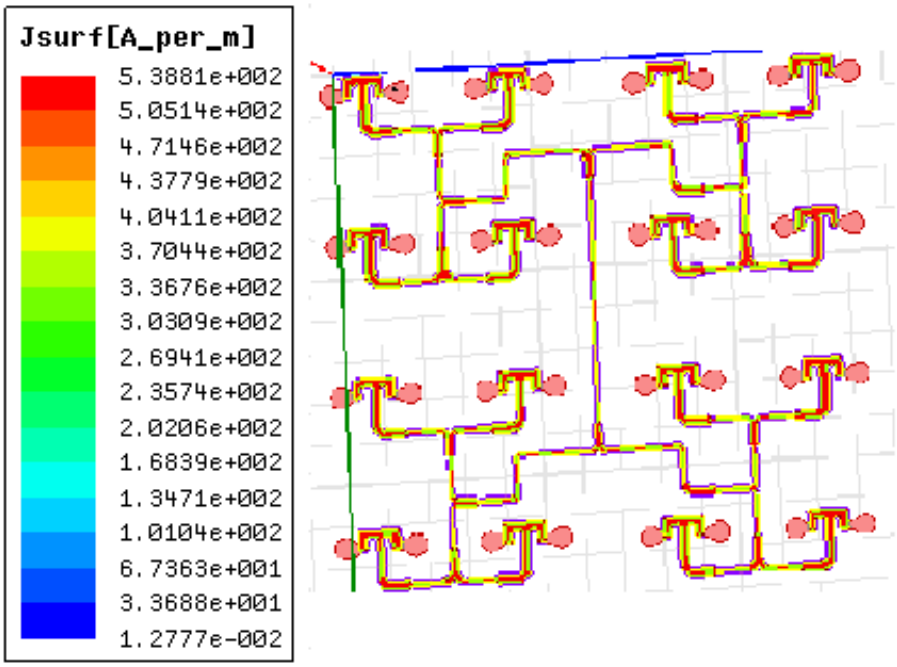

Figure 9. Current density distribution of BFAA

 DOI: https://doi.org/10.30564/jeisr.v3i1.3549

wideband spectrum. Wideband antennas with high efficiency are needed for both cellular access and backhaul networks 19 to cover a wide angular area with a single antenna. We have used HFSS full-wave solver to design the antenna. The dimensions of proposed antenna are mentioned in Table 2 (all dimensions in the Table 2 are in mm).

Table 2. Dimensions of proposed MPWBA

L	W	L1	L2	W1	W2
8	4	1	1	0.5	0.2

The configuration of our designed MPWBA is shown in Figure 10. The antenna is comprised of square shape, three C shaped structures are connected to four sides of square as shown in Figure 10, distance between two C shaped structures are maintained close to _/8. Left and right C shape structures are assumed as input ports. GaN was used as substrate while simulating antenna array. The substrate details which we used while simulating are, thickness of substrate is 1mm, loss tangent value is 0 and relative permittivity is 9.7. The top layer has MPWBA which is embedded in the GaN substrate, which has a distance of 0.1mm to the top surface of the substrate. The bottom layer is assumed as ground. The pink color in Figure 10 is gold material, green color is GaN material and light green color is GaN substrate. Our proposed MPWBA antenna can work with multiple ports, from port 1 to port 12. Our proposed antenna will give best performance with port 7.

The Figure 11 depicts the S11 response of the proposed MPWBA. The proposed MPWBA has return loss of -32 dB with input ports 1 & 2, -46 dB with port 7, and -15dB with remaining ports. The bandwidth of the antenna is

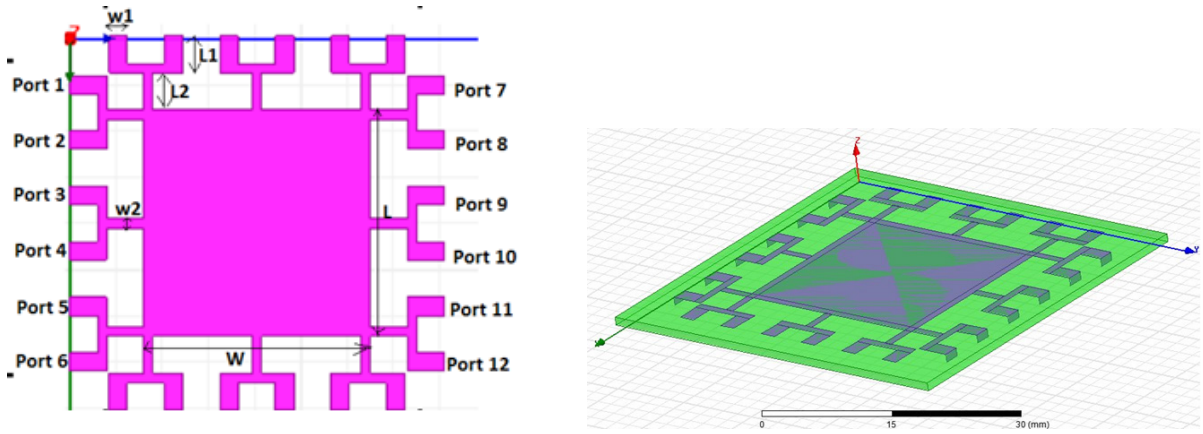

(a) (b)

Figure 10. (a) Geometry of the proposed MPWBA (b)3D top view of MPWBA

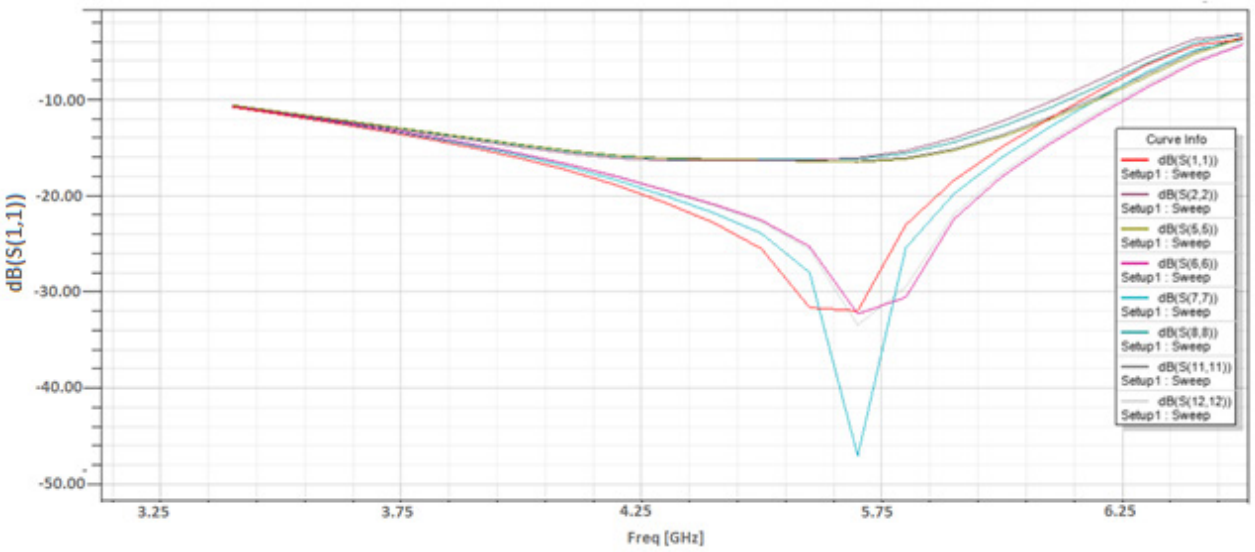

Figure 11. Return loss (S11) response of MPWBA

DOI: https://doi.org/10.30564/jeisr.v3i1.3549

nearly 3 GHz (3.5 GHz to 6.5 GHz).

The Figure 12 shows VSWR (voltage standing wave ratio) of MPWBA, which is nearly 0.75 which is enough for rejecting unwanted signals and to satisfy the bandwidth requirement for specified frequency range. The proposed MPWBA 3D radiation pattern is shown in Figure 13. Our proposed antenna has maximum gain of 7.3 dB. It indicates that very good polarization proposed antenna. The Figure 14a, b are radiation patterns in YZ and XZ directions respectively.

The simulated results of proposed BFAA and MPWBA are mentioned in the below Table 3.

Table 3. Performance comparison table of BFAA and MP-WBA

Content	units		
Antenna type		BFAA	MPWBA
Single antenna size (L*W)	mm*mm	6.3*11.5	8*12
Antenna array size (L*W)	mm*mm	63*67	
Return loss S11	dB	34	46
Antenna gain	dB	8.7	7.3
Peak Directivity	dB	8.9	5.6
Antenna bandwidth	GHz	5.67-5.93	3.5-6.5
Radiated power	dBm	23	20.7
Accepted power	dBm	25	22
Radiation Efficiency	%	93	87
VSWR	GHz	1.2	0.75

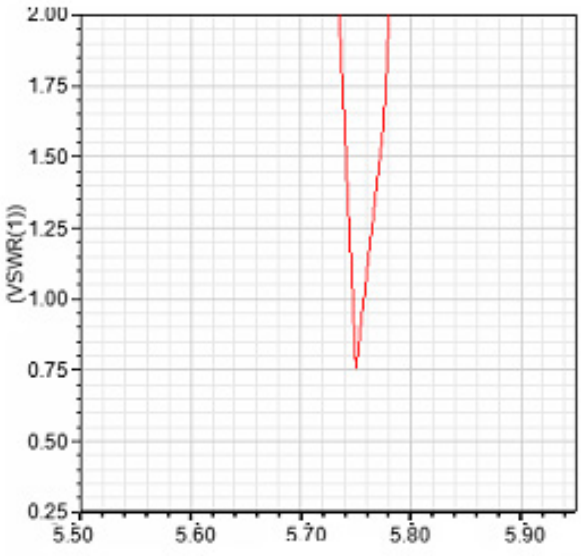

Figure 12. VSWR response of MPWBA

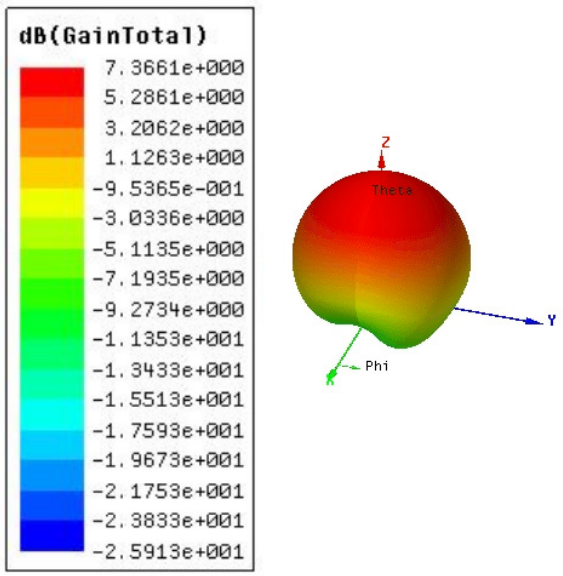

Figure 13. The 3D radiation pattern of proposed MPWBA from HFSS

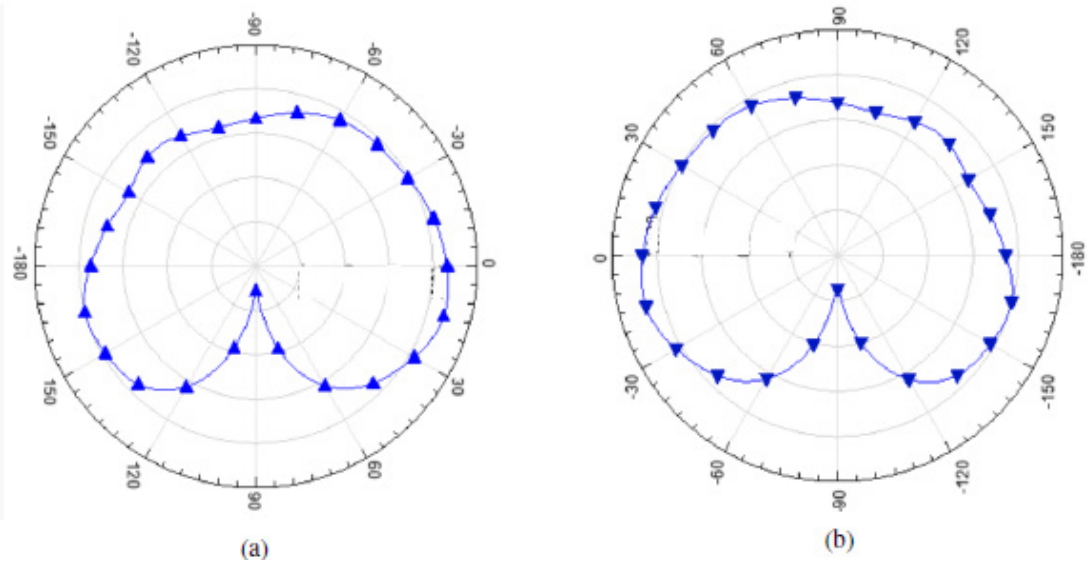

Figure 14. (a) Radiation pattern of proposed antenna in YZ plane (b) Radiation pattern of proposed antenna in XZ plane

 DOI: https://doi.org/10.30564/jeisr.v3i1.3549

5. Impedance Matching Network

In this paper, the power conversion process is proposed at 5.8 GHz frequency. At such frequency, the reflected power occurs when the load impedance is not matched to the characteristic impedance of source impedance. Traditionally spiral inductors are preferred instead of resistors and transmission lines to enhance the thermal noise performance; however, they cannot be used at high frequency because of the self-resonance and stray impedances. In addition, they also occupy a large onchip space. In order to overcome such problems, we adopted a new design strategy in this paper. The proposed approach is based on closed-form and recursive relationships [22]. We calculated stub values using ADS object function to optimize the whole matching networks. During 5.7 GHz to 5.9 GHz, the maximum transducer gain limit to 64dB and the minimum transducer gain is 63dB. As a result, we can get a good transducer curve, whose flatness is less than ±0.2 dB at desired frequency of 5. 8 GHz. Traditionally Network Response is calculated to check the loss value of circuit. So we plotted S11 to find the loss of the network schematic, the S11 value at 5.8 GHz is lower than -10 dB. To investigate circuit stability and perfect match we plotted impedance (Figure 15) on Smith chart as shown in Figure 15.

6. Design and Optimization of Multifunction Filter

As shown in Figure 19, we need two filters for the design of the rectifier circuit. One is at input side and one is at output side. In this paper, we are using our multifunction filter circuit 21. The core LPF circuit with minor changes is converted into BPF and HPF. For BPF a matching network is added at the output of LPF, addition of matching network does not contribute significant loss as evident from the value of S11.

6.1 Low Pass Filter (LPF)

In our proposed filter concept, the number of poles decides range of cut-off frequency of a filter. For example, we designed LPF circuit with cut-off frequency of 5.8 GHz, therefore, we placed 5 poles. To enhance attenuation in the stopband, length and width of the poles of proposed filter are adjusted. P1 and P5 are identical as well as P2 & P4 are identical in length and width. Length of P1 or P5 length of P2 or P4 length of P3. Whereas the Width of poles should be such that width of P3 width of P2 or P4 width of P1 or P5. For microstrip filters optimum distance between poles is also very crucial as this length will act as capacitive or inductive (depending upon the frequency

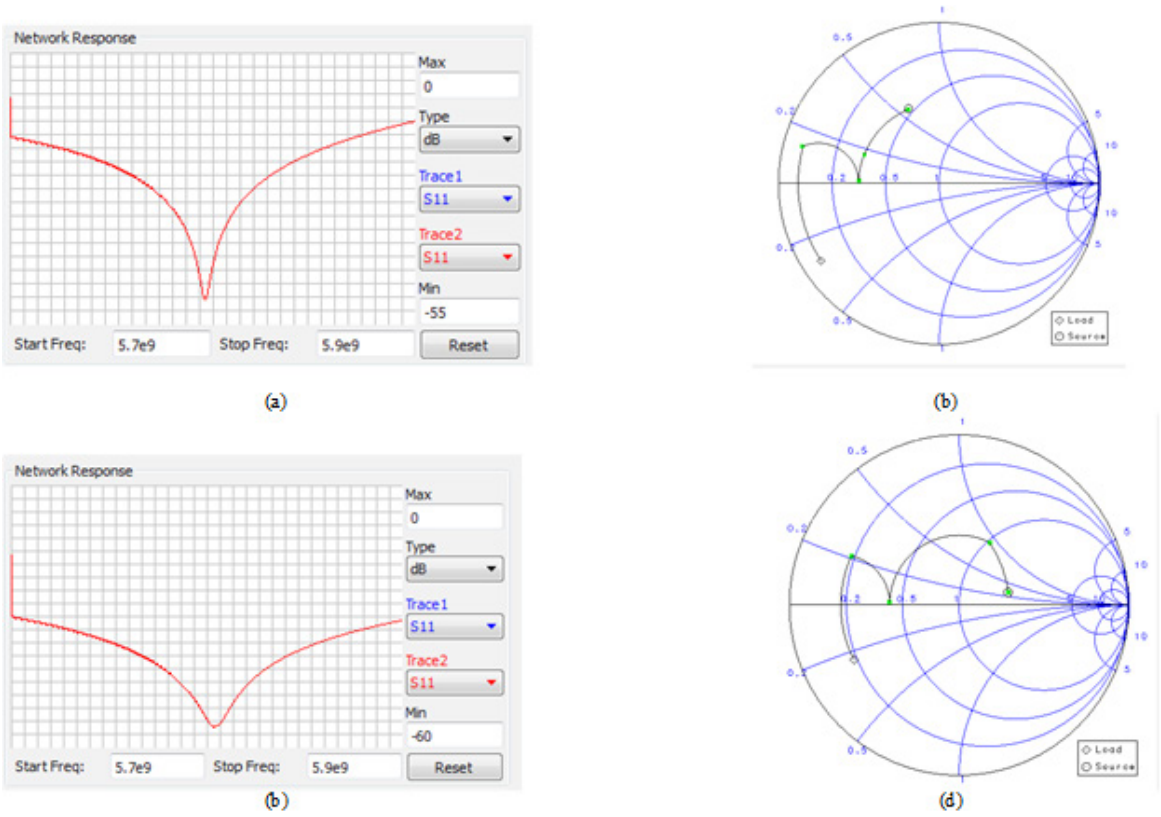

Figure 15. (a) Radiation pattern of proposed antenna in YZ plane (b) Radiation pattern of proposed antenna in XZ plane

DOI: https://doi.org/10.30564/jeisr.v3i1.3549

of operation and distance between poles). The passband frequency could be adjusted via the structure parameters of the poles. The designed multifunction filter is simple in structure and compact in size.

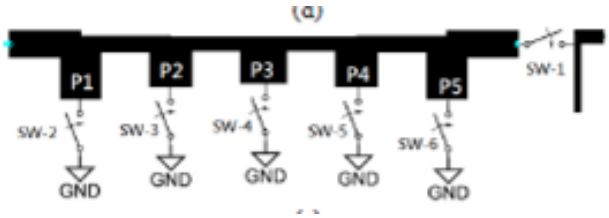

Figure 16. Multimode filter

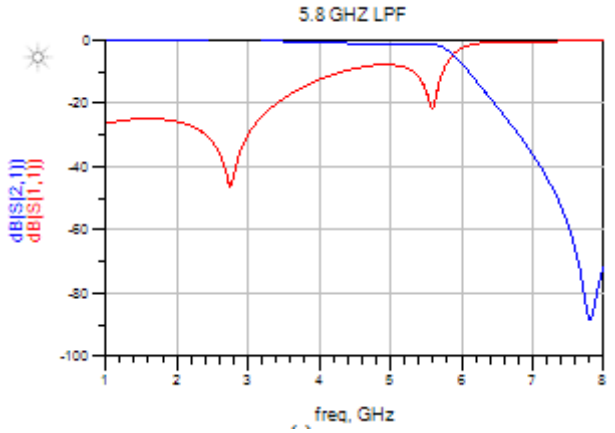

Figure 17. S11 and S21 response of LPF

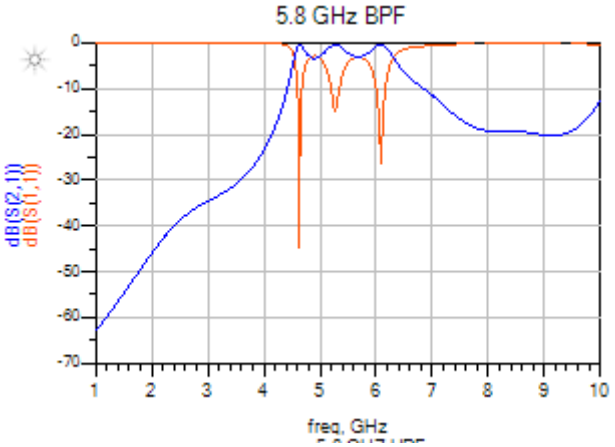

Figure 18. S11 and S21 response of BPF

Figure 17 depicts response of proposed LPF. In case of LPF, simulated -3 dB passband range is obtained from DC to 5.85 GHz. B. Band Pass Filter (BPF). As mentioned above, the LPF circuit with minor changes behaves like BPF. For BPF a matching network is added at the output of LPF. The addition of matching network does not contribute significant loss as evident from the value of S11 (lower than-20 dB). The BPF passband at the desired frequency is realized by adjusting the structure parameters of the matching network. Figure 18, presents simulated of proposed BPF.

7. Rectifier Design

We have used a PNP transistor as a diode while designing the rectifier circuit. Agilent ADS is used for rectifier design with the concept is, 1) To measure the S-parameter values of PNP diode. 2) Design the rectifier circuit according to the Figure 19 by de-embedding the S-parameter values. 3) We have to make sure that the input RF signal should be supplied to rectifier circuit without any significant loss. To achieve this, we have activated LPF from the multifunction filter block using switch1 as shown in Figure 16. 4) Design input matching network between LPF and rectifier. 5) Harmonics are generated during the RF to DC conversion process, which should be removed before collecting the DC power. BPF (is activated from the multifunction filter) is added at rectifier output side to remove unwanted harmonics. Figure 22b shows that even harmonics of rectifiers are attenuated (¡-50dB) at 5.8 GHz frequency with BPF. 6)Optimize the impedance matching network of BPF circuit so that rectifier should give high efficiency with low load resistance values without compromising attenuation of harmonics. 7)Design output matching network between BPF and load.

To investigate the loss of proposed WPT architecture, we have simulated S11 of WPT module chain with BFAA and MPWBA in ADS. The results are shown in Figure 20.

Traditionally S11 is calculated to check the return loss value of circuit. So we plotted S11 to find the loss of the whole architecture (antenna, filter, input matching network, rectifier, output matching network and load) the S11 value at 5.8 GHz is lower than -10dB. Figure 20 indicates that input and matching networks, input and output filter networks are worked well along with the design concepts. Our proposed design has achieved the return loss of about -31.9 dB, -27.8 dB, at 5.8 GHz for BFAA and MPWBA respectively.

To check the performance of rectifier power conversion efficiency (PCE) is an important factor, which denotes how efficiently the rectifier converts the input RF power to DC power. Harmonic balance (HB) simulation is used in ADS to calculate PCE. PCE can be calculated by using

$$PCE = \frac{P_{out}}{P_{RFpower}} * 100 \quad (1)$$

$$P_{out} = \frac{V_{DC}^2}{R_{LOAD}} \quad (2)$$

Figure 21 shows the PCE performance graphs of pro-

 DOI: https://doi.org/10.30564/jeisr.v3i1.3549

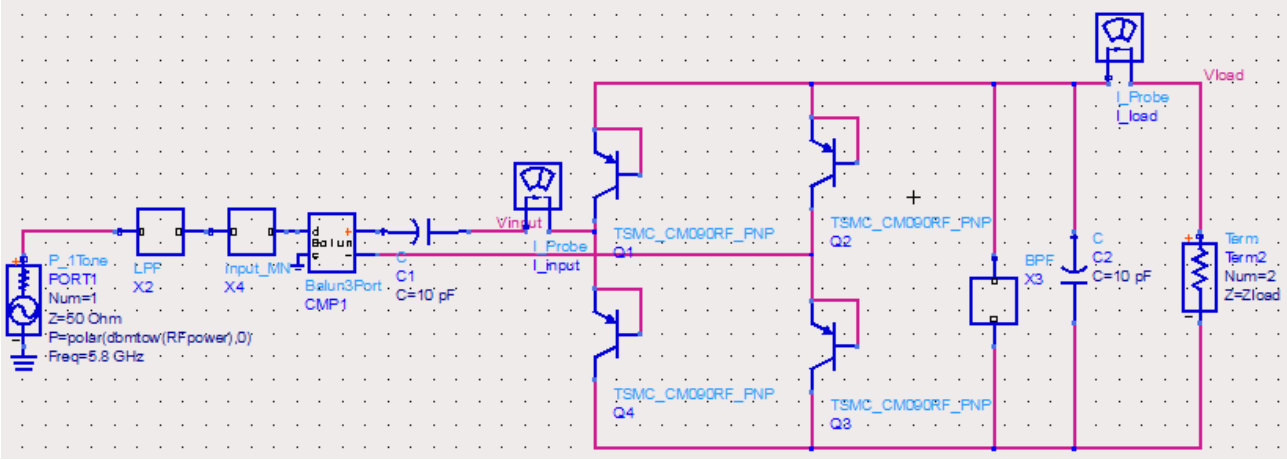

Figure 19. Schematic diagram of proposed rectifier

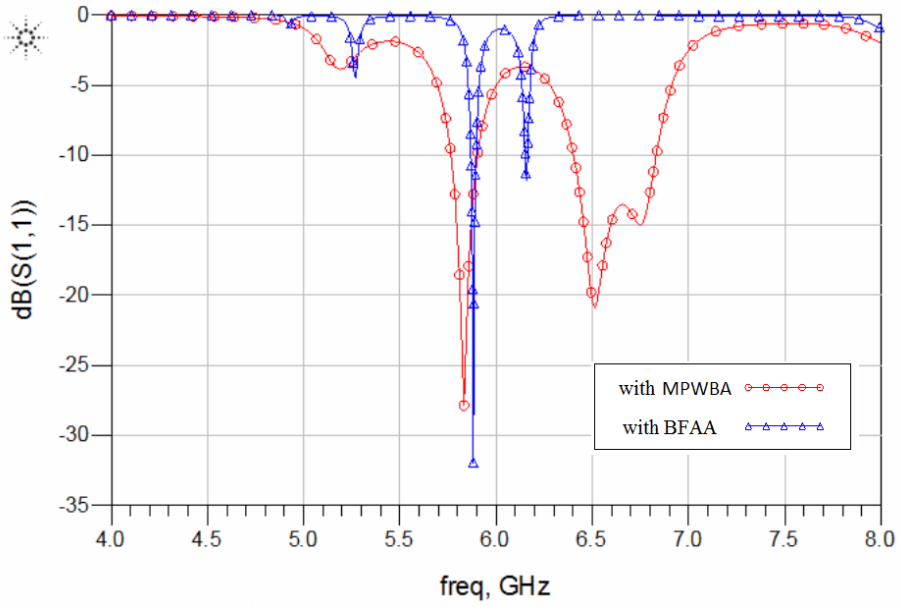

Figure 20. Return loss (S11) of WPT module chain with BFAA and MPWBA

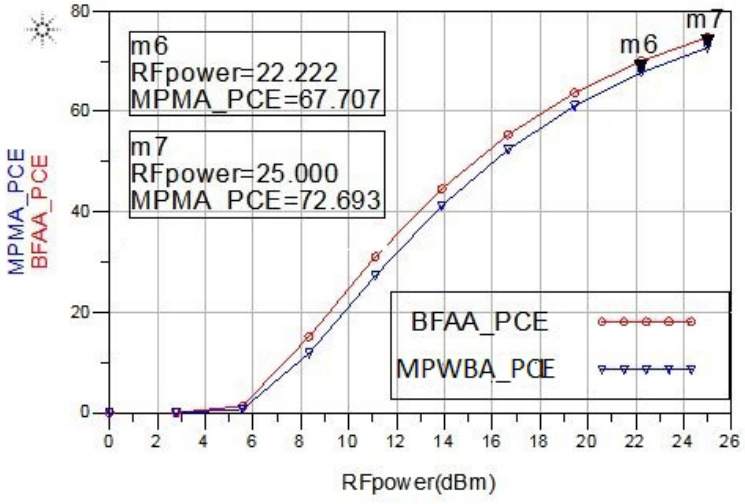

Figure 21. PCE of the proposed rectifier with BFAA and MPWBA

DOI: https://doi.org/10.30564/jeisr.v3i1.3549

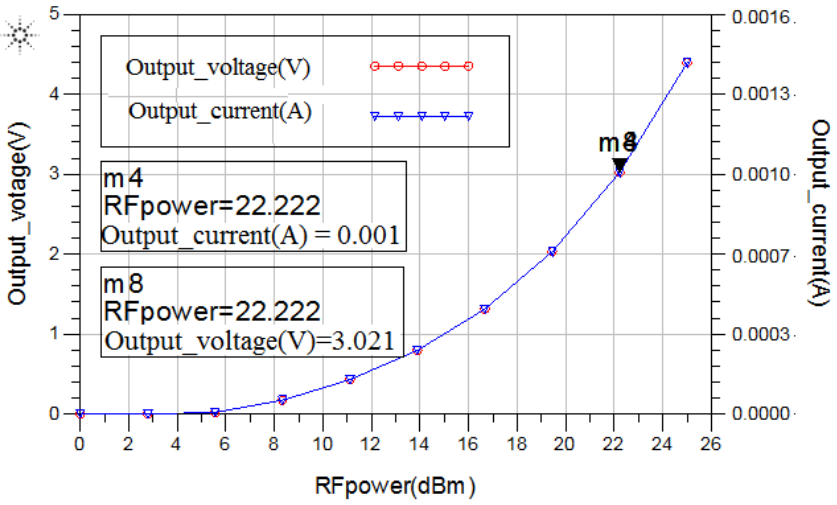

Figure 22. (a) Output voltage graph of rectifier (b) Harmonics of rectifier at 5.8 GHz frequency

Table 4. Design specification comparison of proposed work with previously published works

		[26]	[27]	[28]	[29]	[30]	[31]	[32]	My work	
Year		2005	2010	2011	2013	2015	2016	2017	2021	2021
Frequency	GHz	5.8	2.45	2.45	5.8	5.8	16.5	245	5.8	5.8
Output Voltage	V	3.41	3.64	2.82	0.18	1.41	1.2	5	3	3
Output Current	mA	12	3.46	0.18	0.4	14	-	10	1	1
Conversion Efficiecny	%	68.5	52	63	37	64.8	63	5.5	67	74
Load	Ω	270	1050	50	1000	100	10000	500	80	40

posed rectifiers. The PCE for rectifier with BFA antenna and MPM antenna is 72% and 67%, with an optimal load resistance 40 ohm and 80 ohms respectively. Our rectifier circuit is designed to charge a 5G/6G radio module rechargeable battery of 3 V, 1 mA.

The simulated output DC voltage and current against the input power are shown in Figure 22a. A comparison of performances of proposed work with previously published works from 2005 to 2017 is highlighted in Table 4. Power conversion efficiency is better than previously published papers.

8. Conclusions

The design of a novel WPT module using monolithic components on the GaN substrate is presented in this paper. The WPT module consists of BFAA, PPC, LPF, input matching network, rectifier, and output matching network. logic circuit can be designed and built on substrate or keep it off-chip. We investigated innovative designs for the WPT components with potential for integration on a GaN substrate. Monolithic WPT module shows loss of less than -10 dB at 5.8 GHz which can be further improved with design refinement. To validate our designs, we selected 5.8 GHz ISM band but module design can be easily scaled to millimeter-wave frequencies such as 28 GHz being considered for 5G/6G system. To our knowledge, this first reported design of WPT module on GaN chip. Our proposed module will offer significant SWAP-C advantages. Our proposed rectifier has RF-DC conversion efficiency of 74% and 67% with beam-forming antenna and multiple port antenna respectively. Our WPT module is designed to charge a rechargeable battery (3 V and 1 mA) of a radio module which will be used between two antennas in future 5G/6G networks. In the future, we will extend our proposed technologies to millimeter (mm) wave frequency, as there are several motivations to use mm-wave frequencies in radio links such as availability of wider bandwidth, relatively narrow beam widths, better spatial resolution and small wavelength allowing modest size antennas to have a small beam width.

 DOI: https://doi.org/10.30564/jeisr.v3i1.3549

Acknowledgments

We are thankful to our National Chiao Tung University, Taiwan for providing the facilities to carry out our research.

References

[1] Advanced Antenna Systems for 5G," America, Tech. Rep., 2019.

[2] S. Y. Choi, B. W. Gu, S. W. Lee, W. Y. Lee, J. Huh, and C. T.Rim, "Generalized Active EMF Cancel Methods for Wireless Electric Vehicles," IEEE Transaction on Power Electronics, vol. 29, no. 11, pp.5770-5783, Nov 2014.

[3] S. Y. R. Hui, W. Zhong, and C. K. Lee, "A Critical Review of Recent Progress in Mid-Range Wireless Power Transfer," IEEE Transactions on Power Electronics, vol. 29, no. 9, pp. 4500-4511, Sep 2014.

[4] C. A. Tucker, U. Muehlmann, and M. Gebhart, "Contactless power transmission for NFC antennas in credit-card size format," IET Circuits, Devices and Systems, vol. 11, no. 1, pp. 95-101, 2017.

[5] J. Chu, W. Gu, W. Niu, and A. Shen, "Frequency splitting patterns in wireless power relay transfer," IET Circuits, Devices Systems, vol. 8, no. 6, pp. 561-567, Nov 2014.

[6] W. X. Zhong, C. Zhang, X. Liu, and S. Y. R. Hui, "A Methodology for Making a Three-Coil Wireless Power Transfer System More Energy Efficient Than a Two-Coil Counterpart for Extended Transfer Distance," IEEE Transactions on Power Electronics, vol. 30, no. 2, pp. 933-942, Feb 2015.

[7] J. B. Rosolem, "Powerˆa A ROverˆa€A RFiber Applications for Telecommunications and for Electric Utilities," in Optical Fiber and Wireless Communications. InTech, June 2017.

[8] J. Zhang, X. Ge, Q. Li, M. Guizani, and Y. Zhang, "5G Millimeter-Wave Antenna Array: Design and Challenges," IEEE Wireless Communications, vol. 24, no. 2, pp. 106-112, Apr 2017.

[9] Rajinikanth Yella, Krishna Pande, Ke Horng Chen, Edward Chang 28 GHz Monolithic Transmitter on GaN chip for 5G application. The Tenth International Conference on Advances in Satellite and Space Communications SPACOMM 2018.

[10] Rajinikanth Yella, Krishna Pande, Ke Horng Chen, Edward Chang Design of On-Chip GaN transmitter for wireless communication, International Journal On Advances in Telecommunications 2018.

[11] T. S. Rappaport, Shu Sun, R. Mayzus, Hang Zhao, Y. Azar, K. Wang, G. N. Wong, J. K. Schulz, M. Samimi, and F. Gutierrez, "Millimeter Wave Mobile Communications for 5G Cellular: It Will Work!" IEEE Access, vol. 1, pp. 335-349, 2013.

[12] Q. Luo, S. Gao, N. Carvalho, K. Osipov, J. Wurfl, R. Vilaseca, D. Pham-Minh, A. Marques, J. Pinto, and R. Martins, "GaN-Integrated Beam-Switching High-Power Active Array for Satellite Communications," in 12th European Conference on Antennas and Propagation (EuCAP 2018). Institution of Engineering and Technology, 2018, pp. 621 (5 pp.)-621 (5 pp.).

[13] D. Liu, B. Gaucher, U. Pfeiffer, and J. Grzyb, Eds., Advanced Millimeter-Wave Technologies. Chichester, UK: John Wiley Sons, Ltd, feb 2009.

[14] C. Narayan, Antennas And Propagation. Technical Publications, 2007.

[15] S. Zhang and G. F. Pedersen, "Mutual Coupling Reduction for UWB MIMO Antennas With a Wideband Neutralization Line," IEEE Antennas and Wireless Propagation Letters, vol. 15, pp. 166-169, 2016.

[16] J.-Y. Lee, S.-H. Kim, and J.-H. Jang, "Reduction of Mutual Coupling in Planar Multiple Antenna by Using 1-D EBG and SRR Structures," IEEE Transactions on Antennas and Propagation, vol. 63, no. 9, pp. 4194-4198, Sep 2015.

[17] Q. Li, A. P. Feresidis, M. Mavridou, and P. S. Hall, "Miniaturized Double-Layer EBG Structures for Broadband Mutual Coupling Reduction Between UWB Monopoles," IEEE Transactions on Antennas and Propagation, vol. 63, no. 3, pp. 1168-1171, Mar 2015.

[18] T. Jiang, T. Jiao, and Y. Li, "Array Mutual Coupling Reduction Using LLoading E-Shaped Electromagnetic Band Gap Structures," International Journal of Antennas and Propagation, vol. 2016, pp. 1-9, 2016.

[19] Fan Yang and Y. Rahmat-Samii, "Microstrip antennas integrated with electromagnetic band-gap (EBG) structures: A low mutual coupling design for array applications," IEEE Transactions on Antennas and Propagation, vol. 51, no. 10, pp. 2936-2946, Oct 2003.

[20] W. Liu, Z. N. Chen, and X. Qing, "Metamaterial-Based Low-Profile Broadband Mushroom Antenna," IEEE Transactions on Antennas and Propagation, vol. 62, no. 3, pp. 1165-1172, Mar 2014.

[21] R. HafeziFard, M. Naser-Moghadasi, J. Rashed-Mohassel, and R.-A. Sadeghzadeh Sheikhan, "Mutual Coupling Reduction for Two Closely- Space Meander Line Antennas Using Metamaterial Substrate," IEEE Antennas and Wireless Propagation Letters, vol. 15, pp. 1-1, 2015.

DOI: https://doi.org/10.30564/jeisr.v3i1.3549

[22] Xin Mi Yang, Xue Guan Liu, Xiao Yang Zhou, and Tie Jun Cui, "Reduction of Mutual Coupling Between Closely Packed Patch Antennas Using Waveguided Metamaterials," IEEE Antennas and Wireless Propagation Letters, vol. 11, pp. 389-391, 2012.

[23] P. Simon, "Analysis and Synthesis of Rotman Lenses," in 22nd AIAA International Communications Satellite Systems Conference Exhibit 2004 (ICSSC), no. May. Reston, Virginia: American Institute of Aeronautics and Astronautics, May 2004, pp. 1-11.

[24] E. C. Rajinikanth Yella, Krishna Pande, and Ke Horng Chen, "Design of On-Chip GaN Transmitter for Wireless Communication," International Journal on Advances in Telecommunications, vol. 11, pp. 125-133, 2018.

[25] R. Yella, K. Pande, K. H. Chen, and L.-C. Wang, "Design and Fabrication of Stepped Impedance Multi-Function Filter," International Journal of Electrical and Computer Systems, vol. 4, pp. 1-5, 2018.

[26] C.-H. Chin, Quan Xue, and Chi Hou Chan, "Design of a 5.8-GHz rectenna incorporating a new patch antenna," IEEE Antennas and.

[27] Wireless Propagation Letters, vol. 4, no. 1, pp. 175-178, 2005.

[28] H. Takhedmit, B. Merabet, L. Cirio, B. Allard, F. Costa, C. Vollaire, and O. Picon,"A 2.45-GHz low cost and efficient rectenna," in EuCAP 2010 - The 4th European Conference on Antennas and Propagation. IEEE, 2010, pp. 1-5.

[29] Z. Harouni, L. Cirio, L. Osman, A. Gharsallah, and O. Picon, "A Dual Circularly Polarized 2.45-GHz Rectenna for Wireless Power Transmission," IEEE Antennas and Wireless Propagation Letters, vol. 10, pp. 306-309, 2011.

[30] T. Matsunaga, E. Nishiyama, and I. Toyoda, "5.8-GHz stacked differential mode rectenna suitable for large-scale rectenna arrays," in 2013 Asia-Pacific Microwave Conference Proceedings (APMC). IEEE, Nov 2013, pp. 1200-1202.

[31] P. Lu, X.-S. Yang, J.-L. Li, and B.-Z. Wang, "A Compact Frequency Reconfigurable Rectenna for 5.2- and 5.8-GHz Wireless Power Transmission," IEEE Transactions on Power Electronics, vol. 30, no. 11, pp. 6006-6010, Nov 2015.

[32] C. Wang, K. Zhao, Q. Guo, and Z. Li, "Efficient self-powered convertor with digitally controlled oscillator-based adaptive maximum power point tracking and RF kick-start for ultralow-voltage thermoelectric energy harvesting," IET Circuits, Devices Systems, vol. 10, no. 2, pp. 147-155, Mar 2016.

[33] P. Kundu (Datta), J. Acharjee, and K. Mandal, "Design of an Efficient Rectifier Circuit for RF Energy Harvesting System," international journal of advanced engineering and management, vol. 2, no. 4, p. 94, Apr 2017.

 DOI: https://doi.org/10.30564/jeisr.v3i1.3549